
# A DETERMINATION OF THE PROPERTIES OF THE NEUTRAL INTERMEDIATE VECTOR BOSON Z°

by

THE L3 COLLABORATION

## ABSTRACT

We report the results of first physics runs of the L3 detector at LEP. Based on 2538 hadron events, we determined the mass $m_{Z^0}$ and the width $\Gamma_{Z^0}$ of the intermediate vector boson Z° to be $m_{Z^0}$ = 91.132±0.057 GeV and $\Gamma_{Z^0}$ = 2.588±0.137 GeV. We also determined $\Gamma_{invisible}$ = 0.567±0.080 GeV, corresponding to 3.42±0.48 number of neutrino flavors. We also measured the muon pair cross-section and determined the branching ratio $\Gamma_{\mu\mu}/\Gamma_h$ = 0.056±0.006. The partial width of $Z^\circ \to e^+e^-$ is $\Gamma_{ee}$ = 88±9±7 MeV.



L3 Preprint #001

October 11, 1989

The discovery of the intermediate vector bosons Z° and $W^{\pm}$ [1] at CERN by the UA1 and UA2 collaborations, following the original ideas and efforts of C.Rubbia and S.Van der Meer, is one of the most important advances in elementary particle physics. This discovery lays the foundations for the experimental verification of the unification of the electromagnetic and weak interactions. The electro-weak theory, advanced by Glashow, Weinberg and Salam [2], now known as the Standard Model, predicted the mass and other properties of these intermediate vector bosons. In this Standard Model, the properties of Z° are well defined and can be calculated. For example, the width of Z° is a measure of the number of different kinds of neutrino-like particles in the universe. The mass of Z° is a precise measure of the Weinberg parameter $\sin^2\theta_W$. Similarly, the forward-backward muon charge asymmetry from Z° decays is also a measure of $\sin^2\theta_W$.

In this paper, we report on the first measurement by the L3 collaboration of some of the properties of Z° [3,4] obtained from the newly constructed electron positron collider LEP, at CERN. LEP was completed on time with performances nearly exactly matching expectations, in terms of luminosity (now $>10^{30}/cm^2 \cdot sec$), in terms of reliability (10% down time) and in terms of background in the experimental area (negligible). The data were taken at 7 energies centered at the $Z^0$ mass.

## 1) The L3 Detector

The L3 detector [5] shown in Fig.1 is a $4\pi$ detector with the following major components: surrounding the intersection region is a vertex chamber with single track resolution of about 40μm and double track resolution of about 400μm. The z coordinate is measured by four layers of proportional chambers with a resolution of 500μm. Electromagnetic showers are measured by BGO crystals, each with approximate dimensions of $2x2cm^2$ (entrance side) by 24cm (length) by $3x3cm^2$ (exit side). These crystals provide us with a measured photon and electron coordinate resolution of 1 to 3mm and an energy resolution better than 1% above 2 GeV and of 5% at 100 MeV. The combination of both vertex chamber and BGO information provides clean measurement of inclusive electrons and also enables us to distinguish photons from electrons. Surrounding the BGO, the hadron calorimeter was constructed with uranium plates sandwiched with proportional chambers. It provides a uniform measurement of hadron energy with seven absorption lengths of material. It

measures hadron energy with a resolution of $(55/\sqrt{E}+5)\%$ and $\Delta\Theta = 3.0°$, $\Delta\varphi = 2.5°$. The muon chamber system measures 50 GeV muons with a momentum resolution of 2%. In order to obtain good hadron rejection, the momentum of muons is measured twice: first in the vertex chamber with a value of $P_v$, and second, by the precision muon chambers with a value $P_\mu$. The muon energy loss $\Delta E$ is measured by the sampling calorimeter which also monitors large angle photon radiation. The energy balance, $P_v = \Delta E + P_\mu$, enables us to eliminate hadron decays and hadron punch-throughs from muon signals. The L3 magnet provides a uniform 5.0 kGauss field along the electron positron beam direction. The magnet has a useful inner volume of 12m by 12m by 14m. The large volume of the magnet provides long measuring lever arms. This, together with the precisely constructed muon chambers and support system enables us to measure muon momentum precisely.

For the present analysis, we used the data collected in the following polar angles:

- for the hadron calorimeter, between 25° and 155°
- for the muon chambers, between 35.8° and 144.2°
- for the electromagnetic calorimeter, between 42.4° and 137.6°.

The data from the vertex chamber were not used for this analysis.

## 2) Measurement of Luminosity

The luminosity is measured by eight radial layers of small angle BGO crystals (24.7mrad < $\Theta$ < 68.8mrad) situated on either side of the interaction point, at z=±2.75m. From the center of gravity of the showers, we calculated the $\Theta$ and $\varphi$ impact coordinates of the $e^{\pm}$ on the BGO calorimeters. Fig.2 shows the coplanarity distribution ($\Delta\varphi \equiv \varphi_+ - \varphi_-$) and clearly demonstrates a background free elastic $e^+e^- \to e^+e^-$ Bhabha peak. We used the following cuts to select the Bhabha event candidates [6] :

- $160° < \Delta\varphi < 200°$
- $\Theta_+$ or $\Theta_- > 30.2$mrad
- $E_\pm > 0.25\sqrt{s}$

This definition of the $\Theta$ cut reduces the sensitivity to transverse beam offsets and detector alignment. The value of the $\Theta$ cut corresponds to the boundary between the first two crystal layers and makes the event selection less dependent on the algorithm used to determine the impact coordinates.

To determine the acceptance, $e^+e^- \to e^+e^-(\gamma)$ events were generated using the Monte-Carlo program described in [7]. The generated events were passed through a detector simulation which included effects of energy loss, multiple scattering and showering in the detector materials and the beam pipe. The simulated events were analyzed by the same program used to analyze the data. The accepted cross section contains a small (0.4%) correction from the $e^+e^- \to \gamma\gamma(\gamma)$ process [8]. The systematic uncertainty on this acceptance includes Monte-Carlo statistics (2.5%), internal detector geometry (2.0%), overall detector positioning as well as beam offsets and beam collision angles (1.5%) [9]. We arrive at an overall systematic error of 3.5% on the acceptance.

To assess the systematic effects of the event selection cuts on the integrated luminosity L, these cuts were studied independently. The results are given in Table 1. Clearly, the value of L is very stable for changes of the cuts. If we add in quadrature the maximum change in L for each variable, we estimate a 1.5% systematic uncertainty in L due to the event selection cuts in $\Theta$, $\Delta\varphi$ and E.

**Table 1**

| Event selection variable | | | Sensitivity | | |
|---|---|---|---|---|---|
| $\Theta$(mrad) | $\Delta\varphi$ | E(GeV) | Data | Monte Carlo | $\Delta$L |
| 30.2 | 180°±20° | 0.25$\sqrt{s}$ | | | |
| 32.0 | nominal | nominal | -7.7% | -6.9% | -0.9% |
| 33.8 | " | " | -21.4% | -21.6% | +0.2% |
| 35.6 | " | " | -34.5% | -34.1% | -0.6% |
| 41.1 | " | " | -55.9% | -56.3% | +0.9% |
| nominal | 180°±10° | " | -1.8% | -0.8% | -1.0% |
| " | 180°±30° | " | +0.4% | +0.2% | +0.2% |
| " | nominal | 0.35$\sqrt{s}$ | -3.3% | -2.6% | -0.7% |

**Table 1:** Sensitivity of the Bhabha sample to the event selection cuts $\Theta$, $\Delta\varphi$ and E. The first line lists the nominal cuts; subsequent lines show the percentage change in the selected event samples for the corresponding changes of the cuts. The last column gives the relative change in the integrated luminosity.

Finally, we estimated the efficiency of the luminosity trigger, which required ≥ 20 GeV in both the ±z BGO calorimeters, to be 98±2%. Combined with an event loss of <0.6% due to errors in the hardware decoding, we get a 2.1% trigger uncertainty in L.

Combining the systematic uncertainty in the acceptance (3.5%) with the systematic uncertainty in the event selection (1.5%) and triggering (2.1%), we arrive at a total systematic uncertainty of 4.3%. The number of Bhabha events and the integrated luminosity are listed in Table 2.

In the following sections, we describe the data on hadrons, electrons and muons. The data were analyzed by two independent groups of physicists, each of the groups deciding their own event selection criteria and cuts. The agreement of comparison of final event samples and cross sections gives us confidence in the validity of the data sample and enables us to assign systematic errors in the final numbers.

## 3) Measurement of Hadrons

The event selection for the process $e^+e^- \rightarrow$ hadrons was based entirely on the energy measured in the BGO and hadron calorimeters. The Monte-Carlo distributions were generated by the Lund program, JETSET version 6.3, described in [10]. The generated events were passed through a detector simulation which included effects of energy loss, multiple scattering, interactions and decays in the detector materials and beam pipe. After simulation, the events were analysed by the same program used to analyse the data.

Figures 3 to 6 compare the data and Monte-Carlo distributions in some of the quantities upon which cuts are applied. We define $E_T$ as the total energy measured in the detector, $E_h$ as the energy measured in the hadron

calorimeter, $E_{\parallel}$ as the energy imbalance along the beam direction, $E_{\perp}$ as the transverse energy imbalance, and the number of jets as being that determined by a cluster algorithm applied in the same way to data and Monte-Carlo. We selected events by applying the following:

1. $0.65 < \frac{E_T}{\sqrt{s}} < 1.35$
2. $\frac{E_h}{E_T} > 0.10$
3. $\frac{|E_{\parallel}|}{E_T} < 0.20$
4. $\frac{E_{\perp}}{E_T} < 0.25$
5. Number of jets above 20 GeV $\geq 1$
6. Number of jets above 10 GeV $\geq 2$

These cuts have been applied in the distributions shown. The data and Monte-Carlo agree in all the distributions shown as well as in a wide range of jet variables (thrust, aplanarity, number of jets, $\cos\theta_{jet}$).

With the above criteria, we find an acceptance of 0.76±0.01±0.02 where the first error is statistical and the second systematic. The systematic error on the acceptance has been determined by varying the cuts on Monte Carlo and data. A trigger and data acquisition efficiency of 0.98±0.02 has been determined, giving an overall acceptance of 0.74±0.01±0.03.

The rate of background has been calculated using Monte-Carlo. We find a 1.2±0.2% contamination from $\tau$ pair production and a 0.8±0.2% contamination from electron pair production. Other sources of background are negligible when the above criteria are applied.

The event selection has been checked independently by physicists scanning all events passing much looser cuts. The agreement is within 1%.

Table 2 gives the cross sections for $e^+e^- \rightarrow$ hadrons measured as a function of energy along with the number of hadron events and the luminosity.

The errors on the cross sections given include systematic errors. There is an overall normalization uncertainty of 6% which is not included in the errors quoted in the table. This overall systematic error has been computed by adding the systematic errors from the luminosity determination and the hadron selection in quadrature.

Table 2

| Energy (GeV) | Hadrons | Corrected hadrons | Bhabhas | Luminosity ($nb^{-1}$) | Cross Section (nb) |
|---|---|---|---|---|---|
| 89.26 | 114 | 152.±15. | 1320 | 15.9±0.4 | 9.6±1.0 |
| 90.27 | 344 | 456.±25. | 1942 | 23.9±0.5 | 19.1±1.2 |
| 91.01 | 319 | 420.±24. | 1145 | 14.3±0.4 | 29.4±1.9 |
| 91.27 | 1221 | 1608.±47. | 4427 | 55.6±0.8 | 28.9±1.0 |
| 92.26 | 188 | 246.±18. | 830 | 10.7±0.4 | 23.1±1.9 |
| 92.52 | 107 | 140.±14. | 622 | 8.0±0.3 | 17.4±1.9 |
| 93.27 | 245 | 318.±21. | 2186 | 28.7±0.6 | 11.1±0.8 |
| all | 2538 | | 12472 | 157.1 | |

**Table 2:** Hadron and Luminosity data

The cross sections given in Table 2 are our basic measurements which are fully corrected. To understand the significance of these measurements, we have performed three fits to the data:

1) A fit to the Z° mass within the Standard Model [11,12].
2) A model independent fit to determine the Z° mass, width and branching ratio into hadrons.
3) A fit within the Standard Model to determine the Z° mass and its width into particles, like neutrinos, which are invisible in our detector.

The last two fits were performed using analytic forms for the Z° cross section which have been given by Cahn [13] and by Borrelli et al. [14]. These functions include the initial state radiation in a relativistic Breit-Wigner resonance shape. The two analytic forms give identical fit results. The two analytic expressions reproduce the cross sections of the programs ZBATCH and ZHADRO [11] within 0.5% in the energy range for which we have data if the same values of the mass, width and branching ratios are used.

In the first fit, we assume that the Standard Model correctly predicts the width and branching fractions of the Z°. The only free parameter, aside from the overall normalization which is allowed to vary within the error quoted above, is the mass of the Z°. We find that the mass of the Z° is 91.135±0.057 GeV.

In the second fit, we allow the Z° mass, width and branching ratio into hadrons to vary. The branching ratio is, of course, directly dependent on our overall normalization. From this fit, we find the Z° mass to be 91.132 ±0.057 GeV and the total width to be 2.588±0.137 GeV.

Finally, in the third fit, we determine the number of light neutrinos assuming we know the Z° width into hadrons and into leptons from the Standard Model ($\alpha_s$=0.12, $m_{top}$=60 GeV, $m_{Higgs}$=100 GeV). In this fit, the Z° mass is a free parameter along with the invisible width. The Z° mass is found to be 91.133±0.056 GeV. Note that the value of the mass and its error are quite insensitive to the fitting method used. The invisible width is 0.567±0.080 GeV giving the number of light neutrino flavors of 3.42±0.48. This fit is shown in Fig.7. The curves from the first and second fits are indistinguishable from the curve in Fig.7.

Since this is the beginning of the first physics run of our experiment, we have been rather conservative in our estimates of systematic errors. An estimate of the effect of normalisation uncertainties was obtained by repeating the analysis while setting the systematic errors to zero. In that case, we obtain 3.29±0.22 for the number of neutrino flavors.

The results of all three fits, including $\chi^2$ are summarized in Table 3. The errors on the parameters given in this table include all statistical and systematic errors associated with our experiment. The error on the Z° mass must be increased due to the uncertainty in the absolute normalization of the LEP machine energy. This uncertainty is 0.046 GeV [15]. When added in quadrature with our error of 0.057 GeV, we get an overall error on the Z° mass of 0.073 GeV.

**Table 3**

| Fit | Z° mass (GeV) | Total Width (GeV) | Invisible Width (GeV) | $\chi^2$/DF |
|---|---|---|---|---|
| 1 | 91.135±0.057 | | | 4.7/5 |
| 2 | 91.132±0.057 | 2.588±0.137 | | 3.8/4 |
| 3 | 91.133±0.056 | | 0.567±0.080 | 4.0/4 |

**Table 3:** Summary of fitted results

## 4) Measurement of Electron Pairs

The event selection for the process $e^+e^- \to e^+e^-(\gamma)$ was mainly based on the BGO calorimeter. We selected events by applying independently the two following sets of cuts to our data sample :

a) Two electromagnetic clusters in the BGO calorimeter with a total energy $> 0.7\sqrt{s}$, or

b) The most energetic electromagnetic cluster in BGO having an energy $>0.45\sqrt{s}$ and a second electromagnetic cluster >2 GeV in the opposite direction with an acolinearity angle <25°, and an energy deposition in the hadron calorimeter behind both electromagnetic clusters less than 5 GeV, in order to eliminate $\tau$ contamination.

The two methods have an efficiency of 0.90±0.06 and 0.86±0.06 respectively. The quoted errors are systematic. The systematic error on the efficiency has been determined by varying the cuts on Monte-Carlo and data. We find from Monte-Carlo studies no significant contamination from $\tau$ pair production. Other sources of background, such as $e^+e^- \to \gamma\gamma$, are negligible when the above criteria are applied. The number of events selected by the two methods is in very good agreement, once corrected for their slightly different selection efficiency.

We observed a total number (efficiency corrected) of N = 108±11±8 events during the data taking, out of which 70±9±5 are found at the two energy points very close to the Z° pole (91.01 GeV and 91.27 GeV). These events are

used to derive a cross section for the process $e^+e^- \to e^+e^-(\gamma)$ in the polar angular interval $42° < \Theta < 138°$ at the Z° pole. We find

$$\sigma(e^+e^- \to e^+e^-(\gamma)) = 1.05 \pm 0.13 \pm 0.09 \text{nb}.$$

The first error is purely statistical and the other has been computed by adding the systematic errors from the luminosity determination and the selection efficiency in quadrature.

The measurement of the production cross section for $e^+e^-$ final states at the Z° peak was also used to determine the partial Z° width $\Gamma_{ee}$. In order to include the effects of photon as well as Z° exchange, we used the Monte-Carlo generator BABAMC [16]. We inserted a scale factor multiplying the weak couplings $g_A$ and $g_V$ in the program. We thus determined the predicted number of $e^+e^-$ events inside our acceptance, corresponding to the cuts described above, as a function of the ratio of the width $\Gamma_{ee}$ to the width corresponding to the Standard Model. We find that $\Gamma_{ee}$ = 88±9 (statistical) ±7 (systematic) MeV, where the systematic error includes the uncertainty due to our measured error on the $Z^0$ width. This result compares to the Standard Model prediction of 83.3 MeV, at our measured $Z^0$ mass value of 91.13 GeV. We note that the contribution of pure QED, without the Z° to the accepted cross section is 12% so that the measurement of $\Gamma_{ee}$ is completely dominated by weak effects.

## 5) Measurement of muon pairs

We have determined the ratio of the $Z^0$ width into muon pairs to its width into hadrons. The muon pair selection has been made with four different sets of cuts on muon momentum, vertex position and scintillator timing relative to the beam crossing. With these cuts we select four samples of events, the smallest having 66 muon pairs and the largest having 97. The four event samples when corrected for acceptance of the cuts all give

$$\Gamma_{\mu\mu}/\Gamma_h = 0.056 \pm 0.006$$

within ±0.001. We estimate a systematic error of 4% or 0.002 on the muon selection. From this, we obtain $\Gamma_{\mu\mu}$=92±6 MeV (from our fitted value of $\Gamma_h \cdot \Gamma_{ee}$ and assuming $\Gamma_{ee}=\Gamma_{\mu\mu}$).

With the muon pair data, we have made a determination of the mass and width of the $Z^0$. The data points are shown in Fig.8. Fitting our data only on our muon pairs, we find that $M_Z$=90.77±0.19GeV and that the total width is 1.92±0.53GeV. The fit chi square is 2.3 for 3 degrees of freedom.

## 6) Summary

Thanks to the excellent performance of LEP, we have analysed 2538 hadron events, 95 electron pairs, and 97 muon pairs near the $Z^0$ mass region. With a conservative estimate of our overall normalization uncertainty of 6%, we have measured

| | |
|---|---|
| the mass of the $Z^0$ to be: | $M_{Z^0}$= 91.132±0.057 GeV |
| (not including the 46 MeV machine energy uncertainty) | |
| the width of the $Z^0$ to be: | $\Gamma_{Z^0}$= 2.588±0.137 GeV |
| the invisible width: | $\Gamma_{invisible}$ = 0.567±0.080 GeV |
| Which gives for the number of neutrinos: | 3.42 ±0.48 |
| We also determined independently | $\Gamma_{\mu\mu}$= 92±6 MeV |
| and | $\Gamma_{ee}$= 88±9±7 MeV |

## 7) Acknowledgments

We wish to thank CERN for its hospitality and help. We want particularly to express our gratitude to the LEP division: it is their excellent achievement which made this experiment possible. We acknowledge the support of all the funding agencies which contributed to this experiment.

**The L3 Collaboration:**

B.Adeva[14], O.Adriani[12], M.Aguilar-Benitez[20], H.Akbari[5], J.Alcaraz[20], A.Aloisio[22], G.Alverson[8], M.G.Alviggi[22], Q.An[15], H.Anderhub[33], A.L.Anderson[11], L.Antonov[30], D.Antreasyan[15], A.Arefiev[21], B.Auroy[11], T.Azemoon[3], T.Aziz[7], P.Bagnaia[26], J.A.Bakken[25], L.Baksay[28], R.C.Ball[3], S.Banerjee[7,14,15], J.Bao[5], L.Barone[26], A.Bay[16], U.Becker[11,14], S.Beingessner[4], Gy.L.Bencze[28], G.Bencze[9], J.Berdugo[14,20], P.Berges[11], B.Bertucci[26], B.L.Betev[30], A.Biland[33], R.Bizzarri[14,26], J.J.Blaising[4], P.Blömeke[1], B.Blumenfeld[5], G.J.Bobbink[2], M.Bocciolini[12], W.Böhlen[31], A.Böhm[1], T.Böhringer[18], B.Borgia[26], D.Bourilkov[30], M.Bourquin[16], D.Boutigny[4], J.G.Branson[27], I.C.Brock[24], F.Bruyant[14], J.D.Burger[11], J.P.Burq[19], X.Cai[33], D.Campana[22], C.Camps[1], M.Capell[3], F.Carbonara[22], F.Carminati[12], A.M.Cartacci[12], M.Cerrada[20], F.Cesaroni[26], Y.H.Chang[11], U.K.Chaturvedi[33], M.Chemarin[19], A.Chen[34], C.Chen[6], G.M.Chen[6], H.F.Chen[17], H.S.Chen[6], M.Chen[11], M.L.Chen[3], G.Chiefari[22], C.Y.Chien[5], C.Civinini[12], I.Clare[11], R.Clare[11], G.Coignet[4], N.Colino[20], V.Commichau[1], G.Conforto[12], F.Crijns[2], X.Y.Cui[15], T.S.Dai[11], R.D'Alessandro[12], X.de Bouard[4,†], A.Degré[4], K.Deiters[32], E.Dénes[9], P.Denes[25], F.DeNotaristefani[26], M.Dhina[33], M.Diemoz[26], H.R.Dimitrov[30], C.Dionisi[26], F.Dittus[23], R.Dolin[11], E.Drago[22], T.Driever[2], P.Duinker[2], I.Duran[14,20], A.Engler[24], F.J.Eppling[11], F.C.Erné[2], P.Extermann[16], R.Fabbretti[33], G.Faber[11], S.Falciano[14,26], S.J.Fan[29], M.Fabre[33], J.Fay[19], J.Fehlmann[33], H.Fenker[8], T.Ferguson[24], G.Fernandez[20], F.Ferroni[26], H.Fesefeldt[1], J.Field[16], G.Forconi[16], T.Foreman[2], K.Freudenreich[33], W.Friebel[32], M.Fukushima[11], M.Gailloud[18], Yu.Galaktionov[21], E.Gallo[12], S.N.Ganguli[7], S.S.Gau[34], G.Gavrilov[13], S.Gentile[26], M.Gettner[8], M.Glaubman[8], S.Goldfarb[3], Z.F.Gong[15,17], E.Gonzalez[20], A.Gordeev[21], P.Göttlicher[1], C.Goy[4], G.Gratta[23], A.Grimes[8], C.Grinnell[11,a], M.Gruenewald[23], M.Guanziroli[15], A.Gurtu[7], D.Güsewell[14], H.Haan[1], K.Hangarter[1], S.Hancke[1], M.Harris[14], D.Harting[2], F.G.Hartjes[2], C.F.He[29], A.Heavey[25], T.Hebbeker[1], M.Hebert[27], G.Herten[11], U.Herten[1], A.Hervé[14], K.Hilgers[1], H.Hofer[33], L.S.Hsu[34], G.Hu[15], G.Q.Hu[29], B.Ille[19], M.M.Ilyas[15], V.Innocente[22], E.Isiksal[33], E.Jagel[15], B.N.Jin[6], L.W.Jones[3], M.Jongmanns[33], H.Jung[33], P.Kaaret[25], R.A.Khan[33], Yu.Kamyshkov[21],

D.Kaplan[8], W.Karpinski[1], Y.Karyotakis[4], V.Khoze[13], D.Kirkby[23], W.Kittel[2], A.Klimentov[21], P.F.Klok[2], M.Kollek[1], M.Koller[31], A.C.König[2], O.Kornadt[1], V.Koutsenko[21], R.W.Kraemer[24], V.R.Krastev[30], W.Krenz[1], A.Kuhn[31], A.Kunin[21], S.Kwan[8], G.Landi[12], K.Lanius[32], D.Lanske[1], S.Lanzano[22], J.M.Le Goff[14], P.Lebrun[19], P.Lecomte[33], P.Lecoq[14], P.Le Coultre[33], I.Leedom[8], L.Leistam[14], R.Leiste[32], J.Lettry[33], X.Leytens[2], C.Li[17], H.T.Li[6], J.F.Li[15], L.Li[33], P.J.Li[29], X.G.Li[6], J.Y.Liao[29], R.Liu[15], Y.Liu[15], Z.Y.Lin[17], F.L.Linde[24], B.Lindemann[1], D.Linnhöfer[14], W.Lohmann[32], S.Lökös[28], E.Longo[26], Y.S.Lu[6], J.M.Lubbers[2], K.Lübelsmeyer[1], C.Luci[14], D.Luckey[11,15,b], L.Ludovici[26], X.Lue[33], L.Luminari[26], W.G.Ma[17], M.MacDermott[33], R.Magahiz[28], M.Maire[4], P.K.Malhotra[7], A.Malinin[21], C.Mana[14,20], D.N.Mao[3], Y.F.Mao[6], M.Maolinbay[33], P.Marchesini[15], A.Marchionni[12], J.P.Martin[19], L.Martinez[20], H.U.Martyn[1], F.Marzano[26], G.G.G.Massaro[2], T.Matsuda[11,c], K.Mazumdar[7], P.McBride[10], Th.Meinholz[1], M.Merk[2], R.Mermod[16], L.Merola[22], M.Meschini[12], W.J.Metzger[2], Y.Mi[15], M.Micke[1], U.Micke[1], G.B.Mills[3], Y.Mir[15], G.Mirabelli[26], J.Mnich[1], M.Moeller[1], L.Montanet[14], B.Monteleoni[12], G.Morand[16], R.Morand[4], S.Morganti[26], V.Morgunov[21], R.Mount[23], E.Nagy[9,14], M.Napolitano[22], H.Newman[23], L.Niessen[1], W.D.Nowak[32], J.Onvlee[2], J.Ossmann[16], D.Pandoulas[1], G.Paternoster[22], S.Patricelli[22], Y.J.Pei[1], Y.Peng[2], D.Perret-Gallix[4], J.Perrier[16], E.Perrin[16], A.Pevsner[5], M.Pieri[12], V.Pieri[12], P.A.Piroué[25], V.Plyaskin[21], M.Pohl[33], V.Pojidaev[21], C.L.A.Pols[2], N.Produit[16], P.Prokofiev[13], J.M.Qian[11,15], R.Raghavan[7], P.Razis[33], K.Read[25], D.Ren[33], Z.Ren[15], S.Reucroft[8], A.Ricker[1], T.Riemann[32], C.Rippich[24], S.Rodriguez[20], B.P.Roe[3], G.Rahal-Callot[33], M.Röhner[1], S.Röhner[1], L.Romero[20], J.Rose[1], S.Rosier-Lees[4,14], Ph.Rosselet[18], J.A.Rubio[14,20], W.Ruckstuhl[16], H.Rykaczewski[33], M.Sachwitz[32], J.Salicio[20], M.Sassowsky[1], G.Sauvage[4], A.Savin[21], V.Schegelsky[13], A.Schetkovsky[13], P.Schmitt[10], D.Schmitz[1], P.Schmitz[1], M.Schneegans[4], M.Schöntag[1], D.J.Schotanus[2], H.J.Schreiber[32], R.Schulte[1], A.Schultz von Dratzig[1], K.Schultze[1], J.Schütte[10], J.Schwenke[1], G.Schwering[1], C.Sciacca[22], P.G.Seiler[33], J.C.Sens[2], I.Sheer[27], V.Shevchenko[21], S.Shevchenko[21], X.R.Shi[24], K.Shmakov[21], V.Shoutko[21], E.Shumilov[21], R.Siedling[1], N.Smirnov[13], A.Sopczak[27], V.Souvorov[13], C.Souyri[4], T.Spickermann[1], B.Spiess[31], P.Spillantini[12], R.Starosta[1], M.Steuer[11,b],

D.P.Stickland[25], B.Stöhr[33], H.Stone[16], K.Strauch[10], K.Sudhakar[7], R.L.Sumner[25], H.Suter[33], R.B.Sutton[24], A.A.Syed[15], X.W.Tang[6], E.Tarkovsky[21], A.Tavenrath[1], J.M.Thenard[4], E.Thomas[15], C.Timmermans[2], Samuel C.C.Ting[11], S.M.Ting[11], Y.P.Tong[34], M.Tonutti[1], S.C.Tonwar[7], J.Tòth[9], K.L.Tung[6], J.Ulbricht[31], L.Urbàn [9], U.Uwer[1], E.Valente[26], R.T.Van de Walle[2], H.van der Graaf[2], I.Vetlitsky[21], G.Viertel[33], P.Vikas[15], M.Vivargent[4], H.Vogel[24], H.Vogt[32], S.Volkov[13], I.Vorobiev[21], A.Vorobyov[13], L.Vuilleumier[18], W.Walk[14], W.Wallraff[1], C.Y.Wang[17], G.H.Wang[24], J.H.Wang[6], Q.F.Wang[10], X.L.Wang[17], Y.F.Wang[12], Z.M.Wang [15,17], J.Weber[33], R.Weill[18], T.J.Wenaus[11], J.Wenninger[16], M.White[11], R.Wilhelm[2], C.Willmott[20], F.Wittgenstein[14], D.Wright[25], R.J.Wu[6], S.L.Wu[15], S.X.Wu[11,15], Y.G.Wu[6], B.Wyslouch[11,14], Z.Z.Xu[17], Z.L.Xue[29], D.S.Yan[29], B.Z.Yang[17], C.G.Yang[6], K.S.Yang[6], Q.Y.Yang[6], Z.Q.Yang[29], Q.Ye[15], C.H.Ye[11,d], S.C.Yeh[34], Z.W.Yin[29], Z.M.You[15], C.Zabounidis[8], L.Zehnder[33], M.Zeng[15], Y.Zeng[1], D.Zhang[27], D.H.Zhang[2], S.Y.Zhang[6], Z.P.Zhang[17], J.F.Zhou[1], R.Y.Zhu[23], A.Zichichi[14,15], J.Zoll[14].

---

[1] 1. Physikalisches Institut, RWTH, Aachen, Federal Republic of Germany[α]
3. Physikalisches Institut, RWTH, Aachen, Federal Republic of Germany[α]

[2] National Institute for High Energy Physics, NIKHEF, Amsterdam; NIKHEF-H and University of Nijmegen, Nijmegen, The Netherlands

[3] University of Michigan, Ann Arbor, United States of America

[4] Laboratoire de Physique des Particules, LAPP, Annecy, France

[5] Johns Hopkins University, Baltimore, United States of America

[6] Institute of High Energy Physics, IHEP, Beijing, People's Republic of China

[7] Tata Institute of Fundamental Research, Bombay, India

[8] Northeastern University, Boston, United States of America

[9] Central Research Institute for Physics of the Hungarian Academy of Sciences, Budapest, Hungary

[10] Harvard University, Cambridge, United States of America

[11] Massachusetts Institute of Technology, Cambridge, United States of America

[12] INFN Sezione di Firenze and University of Firenze, Italy

[13] Leningrad Nuclear Physics Institute, Gatchina, Soviet Union

[14] European Laboratory for Particle Physics, CERN, Geneva, Switzerland
[15] World Laboratory, FBLJA Project, Geneva, Switzerland
[16] University of Geneva, Geneva, Switzerland
[17] Chinese University of Science and Technology, USTC, Hefei, People's Republic of China
[18] University of Lausanne, Lausanne, Switzerland
[19] Institut de Physique Nucléaire de Lyon, IN2P3-CNRS/Université Claude Bernard, Villeurbanne, France
[20] Center of Energy and Environmental Research, CIEMAT, Madrid, Spain[β]
[21] Institute of Theoretical and Experimental Physics, ITEP, Moscow, Soviet Union
[22] INFN-Sezione di Napoli and University of Naples, Italy
[23] California Institute of Technology, Pasadena, United States of America
[24] Carnegie Mellon University, Pittsburgh, United States of America
[25] Princeton University, Princeton, United States of America
[26] INFN-Sezione di Roma and University of Roma, "La Sapienza", Italy
[27] University of California, San Diego, United States of America
[28] Union College, Schenectady, United States of America
[29] Shanghai Institute of Ceramics, SIC, Shanghai, People's Republic of China
[30] Central Laboratory of Automation and Instrumentation, CLANP, Sofia, Bulgaria
[31] Paul Scherrer Institut, PSI, Würenlingen, Switzerland
[32] High Energy Physics Institute, Zeuthen-Berlin, German Democratic Republic
[33] Eidgenössische Technische Hochschule, ETH Zürich, Switzerland
[34] National Science Council, Taiwan, China

[a] also LAA
[b] also Bologna
[c] also KEK
[d] also Nanjing
[†] deceased
α Supported by the German Bundesministerium für Forschung und Technologie
β Partly supported by the grant CCA-8411/129 from the "US-Spain joint committee, Science and Technology program".

## References

[1] UA1 Collaboration :
G. Arnison et al., Phys. Lett. 122B, (1983) 103.
G. Arnison et al., Phys. Lett. 126B, (1983) 398.
C. Albajar et al., Preprint CERN-EP/88-168.
UA2 Collaboration :
P. Bagnaia et al., Phys. Lett. 129B (1983) 130.
R. Ansari et al., Phys. Lett. 186B (1987) 440.

[2] S.L. Glashow, Nucl. Phys, 22 (1961) 579.
S. Weinberg, Phys. Rev. Lett., 19 (1967) 1264.
A. Salam, Elementary Particle Theory, Ed. N.Svartholm, Stockholm, "Almquist and Wiksell" (1968), 367.

[3] G.S. Abrams et al., Phys. Rev. Lett. 63 (1989) 724.

[4] F. Abe et al., Phys. Rev. Lett. 63 (1989) 720.

[5] The Construction of the L3 Experiment, L3 Collaboration, submitted to Nuclear Instruments and Methods, 1989.

[6] J.F. Crawford et al., NIM 127 (1975) 173.

[7] BHLUMI, Version 1.2, June 1988, S. Jadach and B.F.L. Ward.

[8] F.A. Berends, R. Kleiss, Nucl. Phys. B186 (1981) 22.

[9] M. Athanas et al., "Normalization at L3", CERN-88-06, Vol.2 (1988) 119.

[10] T.Sjöstrand and M.Bergtsson, Computer Physics Communic. 43 (1987) 367.

[11] G. Burgers : preprint CERN-TH, 5119/88; also in CERN 88-06, p.121, edited by G. Alexander et al.

[12] D.Y. Bardin et al., CERN Report 89-08.
D.Y. Bardin et al., Phys. Lett. 206B (1988) 539.

[13] R.N. Cahn, Phys. Rev. D36 (1987) 2666.

[14] A. Borrelli et al., preprint CERN-TH, 5441/89.

[15] Machine Group LEP Division, CERN (private communication).

[16] BABAMC, R. Kleiss, F.A. Berends and W. Hollik, "Proceedings of the Workshop on Z physics at LEP, edited by G. Altarelli, R. Kleiss and C. Verzegnassi, CERN Report 89-08, Vol III, 1.

**Figure Captions**

Fig.1 Schematic view of the L3 detector.

Fig.2 An example of the $\Delta\varphi$ distribution of the Bahaba events in the luminosity monitor. The arrows indicate the $160° < \Delta\varphi < 200°$ cut.

Fig.3 Distribution of observed total energy $E_T$ normalized to $\sqrt{s}$ compared with Monte-Carlo for hadron events. The overall energy resolution is 12%.

Fig.4 Distribution of observed relative hadronic energy $E_h/E_T$ compared with Monte-Carlo.

Fig.5 Distribution of observed energy imbalance parallel to the beam direction ($|E_{\parallel}|$) normalized to the observed total energy $E_T$ compared with Monte-Carlo.

Fig.6 Distribution of observed energy imbalance perpendicular to the beam direction ($E_{\perp}$) normalized to the observed total energy $E_T$ compared with Monte-Carlo.

Fig.7 Measured cross section for $e^+e^- \to$ hadrons as a function of $\sqrt{s}$. Data are shown with statistical errors only. The curve shows a fit to the Cahn formula [13] in which $M_{Z^\circ}$ and $\Gamma_{\text{invisible}}$ were left free. The normalization was floated within the quoted 6% systematic error. The widths $\Gamma_{ee}$, $\Gamma_{\mu\mu}$, $\Gamma_{\tau\tau}$ and $\Gamma_{\text{hadrons}}$ were taken from the Standard Model.

Fig.8 Measured cross-section for $e^+e^- \to \mu^+\mu^-$ as a function of $\sqrt{s}$. The solid line is the Standard Model fit. Data are shown with statistical errors only.

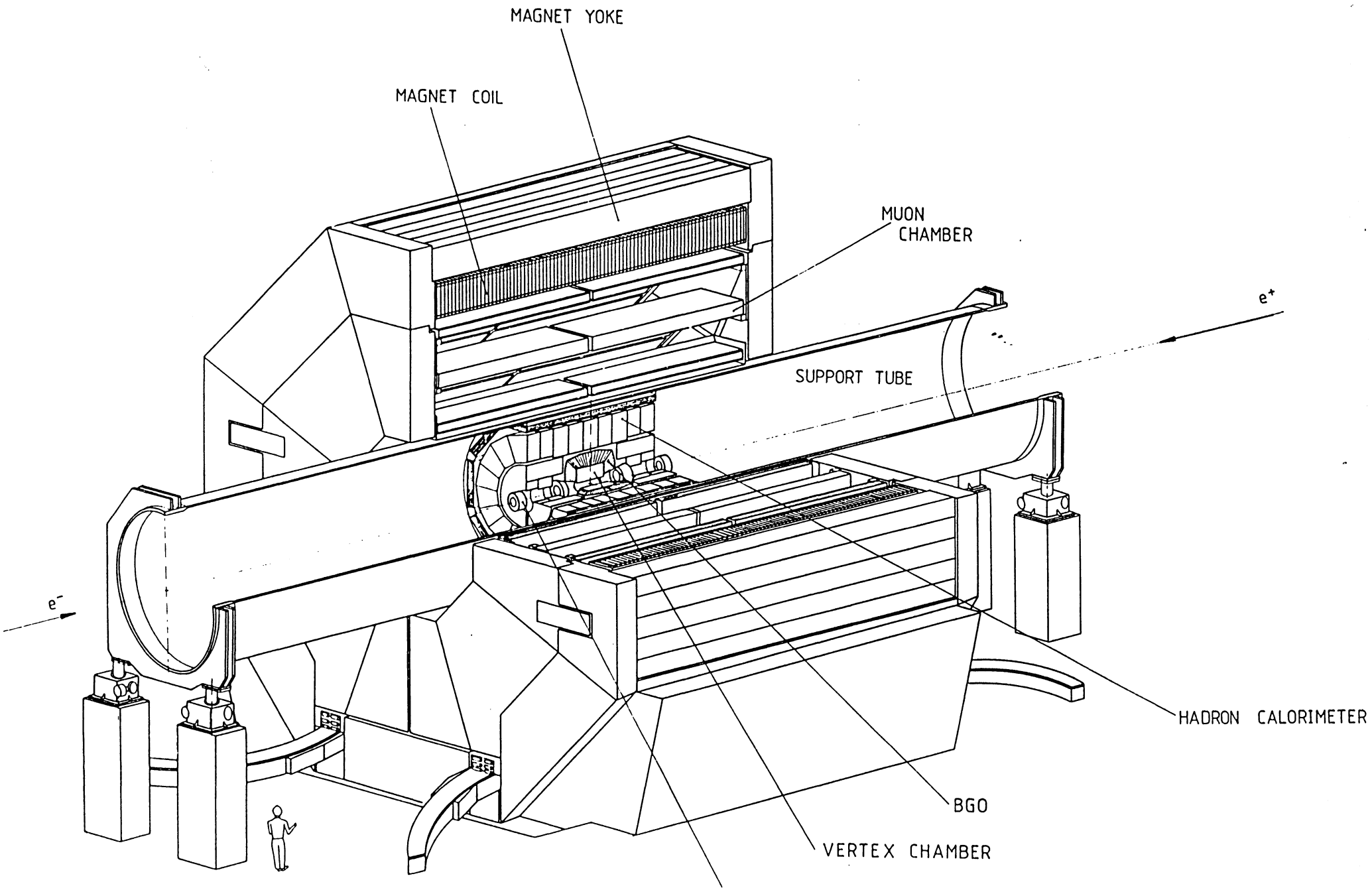
MAGNET YOKE
MAGNET COIL
MUON CHAMBER
e+
SUPPORT TUBE
e-
HADRON CALORIMETER
BGO
VERTEX CHAMBER
LUMINOSITY MONITOR

**Figure 1**

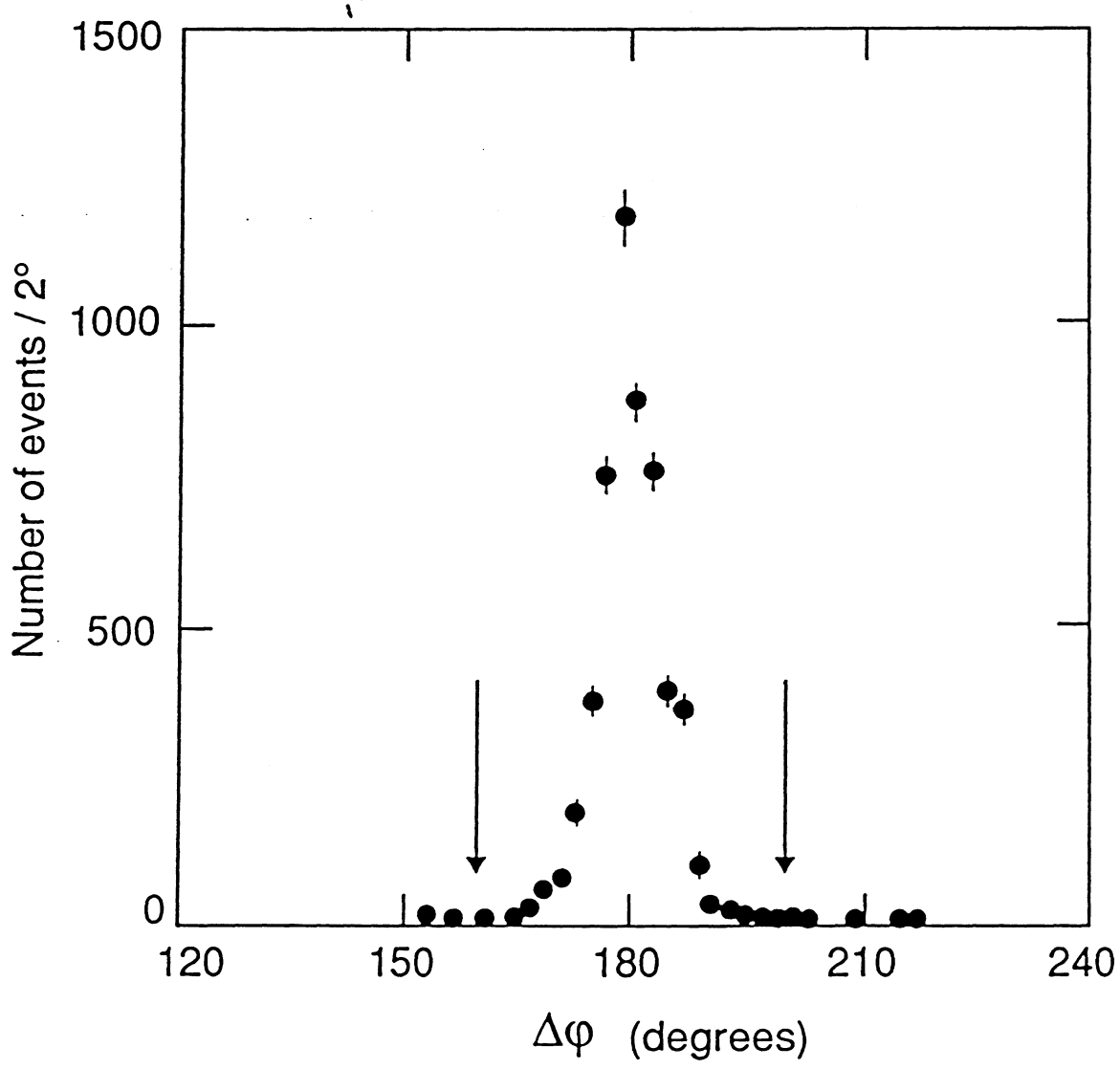
1500
1000
500
0
Number of events / 2°
120
150
180
210
240
Δφ (degrees)

**Figure 2**

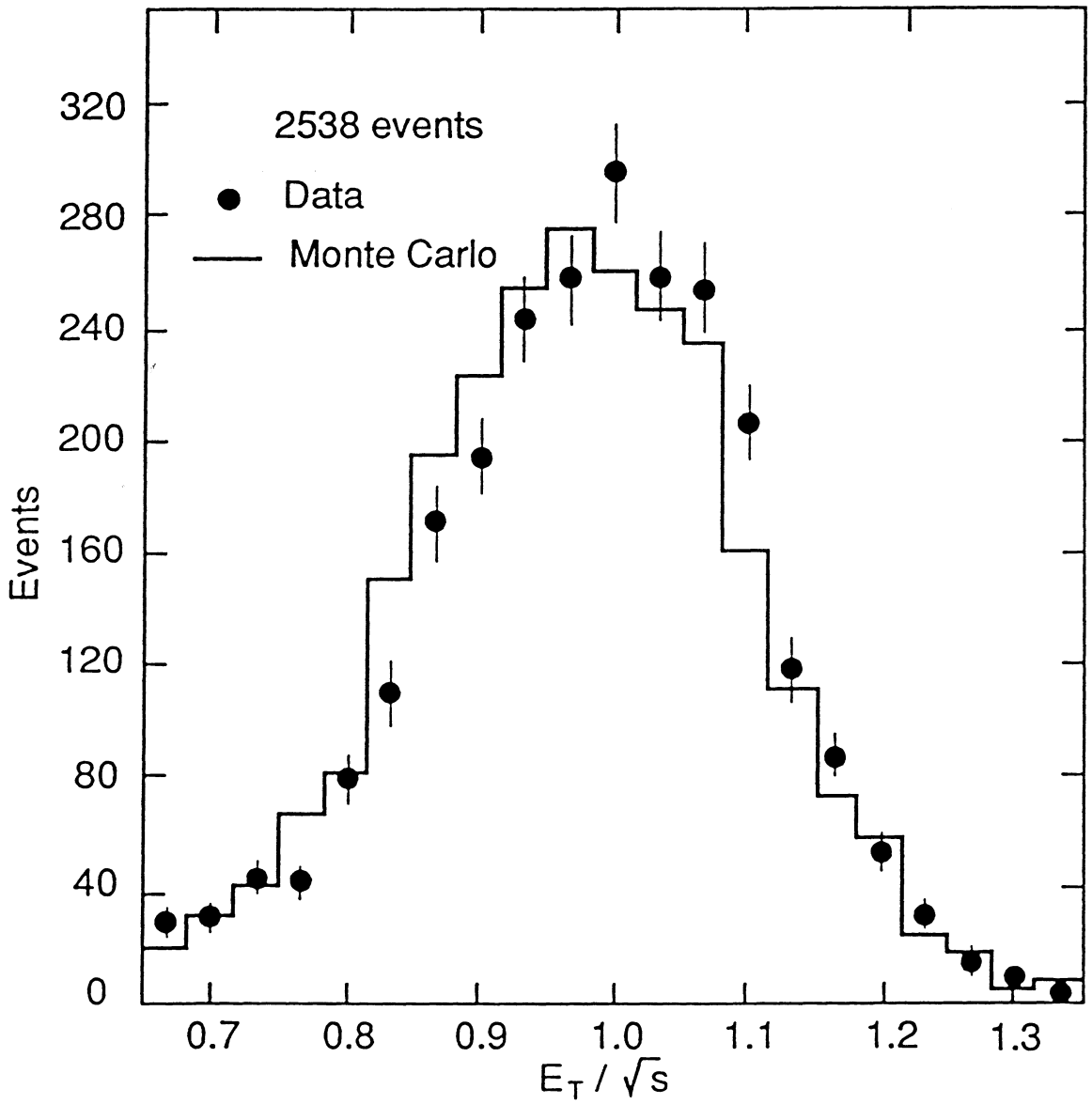
2538 events
Data
Monte Carlo
Events
320
280
240
200
160
120
80
40
0
0.7
0.8
0.9
1.0
1.1
1.2
1.3
$E_T / \sqrt{s}$

**Figure 3**

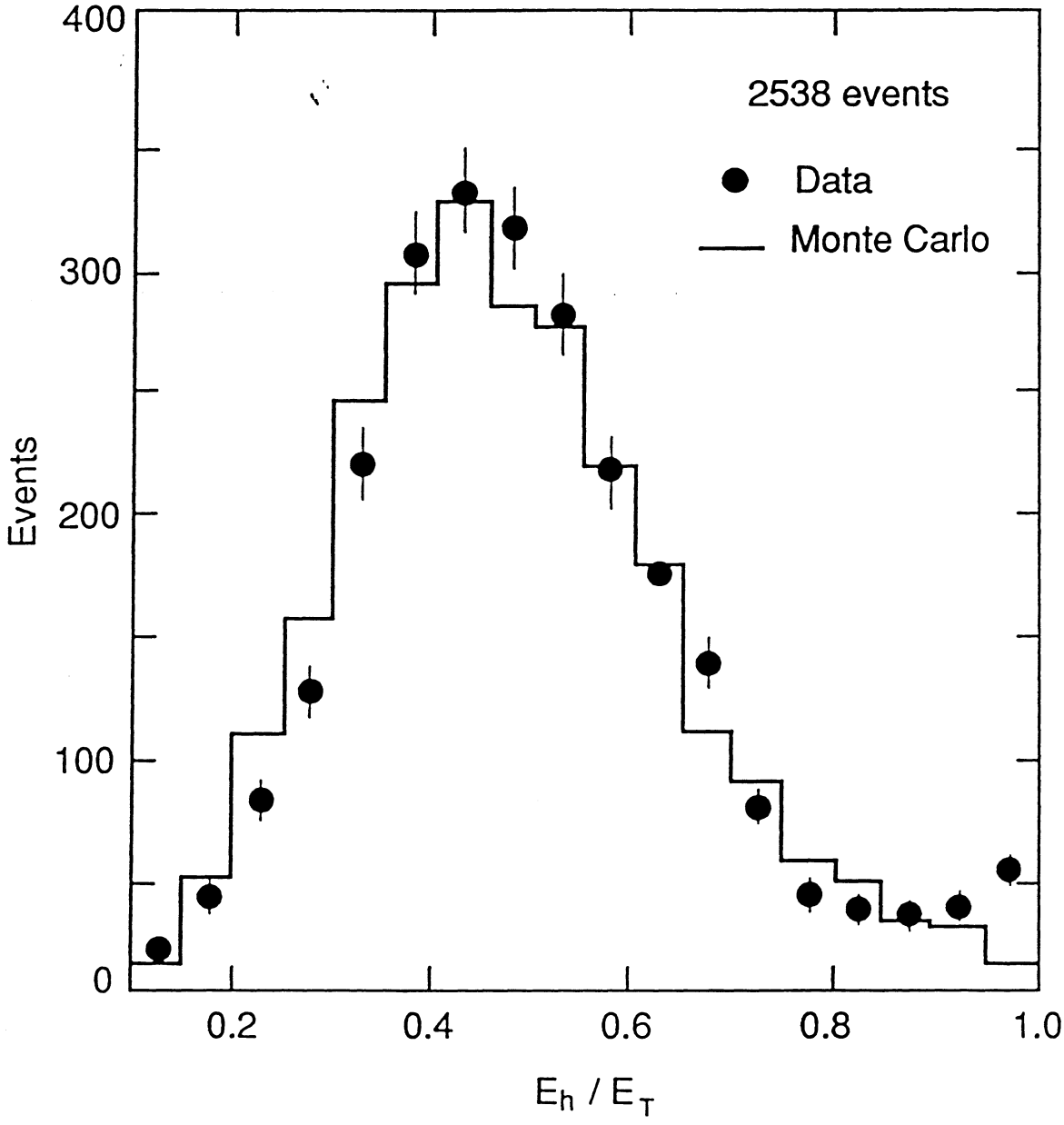
400
300
200
100
0
Events
2538 events
Data
Monte Carlo
0.2
0.4
0.6
0.8
1.0
$E_h / E_T$

**Figure 4**

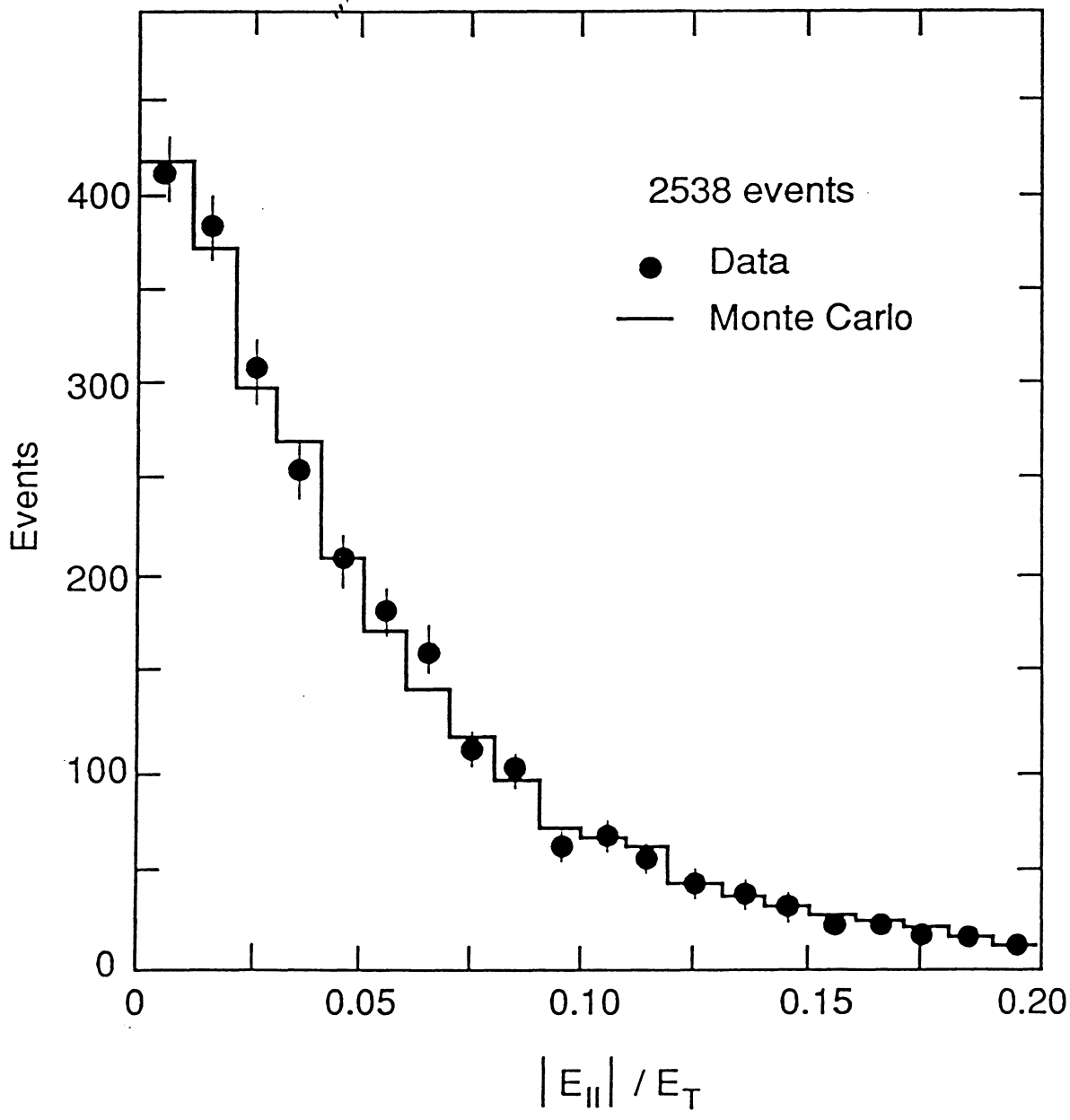
2538 events
Data
Monte Carlo
Events
400
300
200
100
0
0
0.05
0.10
0.15
0.20
$|E_{II}| / E_T$

**Figure 5**

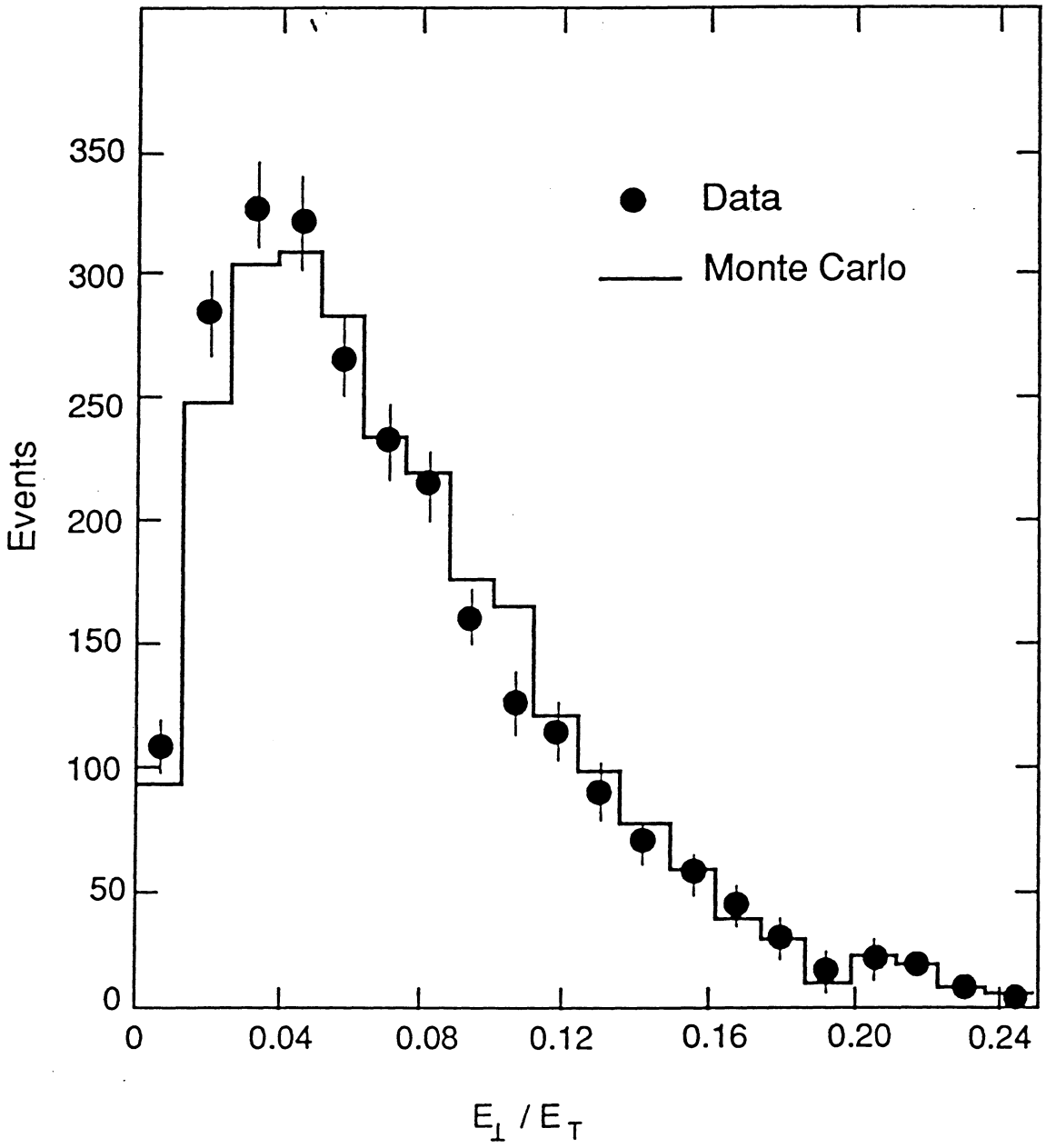
Data
Monte Carlo
Events
350
300
250
200
150
100
50
0
0
0.04
0.08
0.12
0.16
0.20
0.24
$E_\perp / E_T$

**Figure 6**

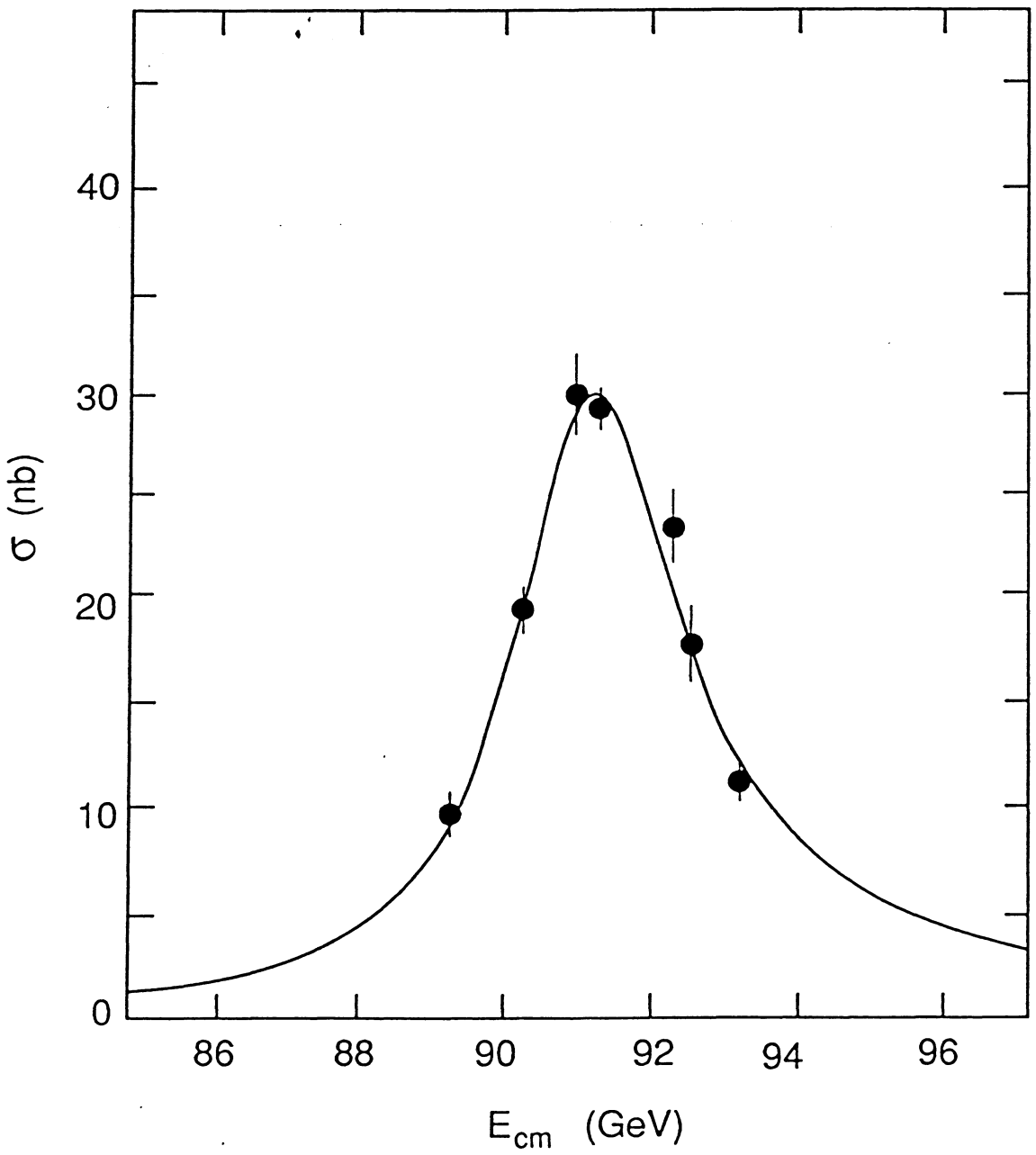


**Figure 7**

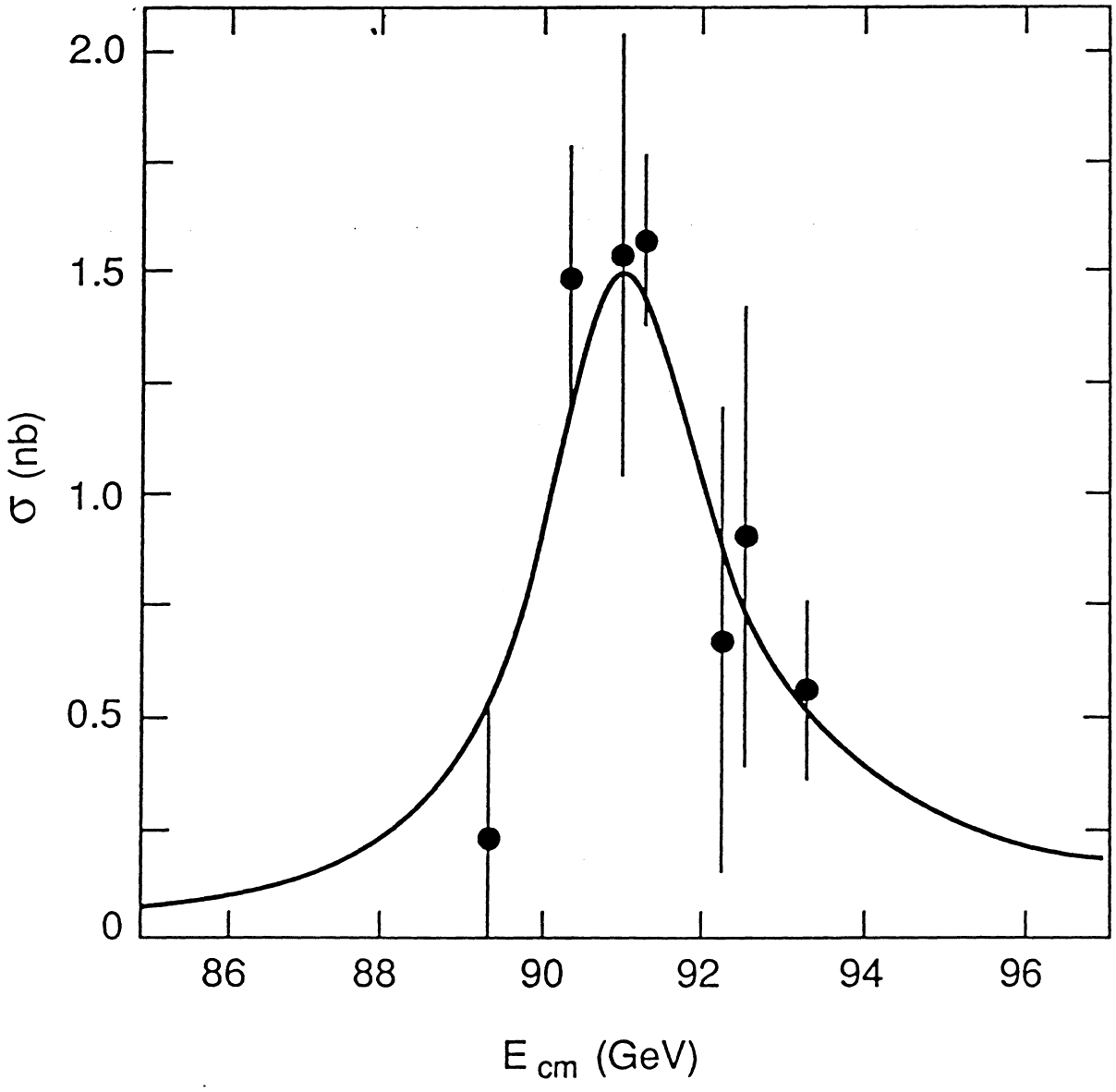


**Figure 8**